

# First principles study of Li diffusion in I-Li<sub>2</sub>NiO<sub>2</sub> structure

Kisuk Kang,<sup>1,2,\*</sup> Dane Morgan,<sup>3</sup> and Gerbrand Ceder<sup>4</sup>

<sup>1</sup>Department of Materials Science and Engineering, KAIST, 335 Gwahangno, Yuseong-gu, Daejeon 305-701, Republic of Korea

<sup>2</sup>KAIST Institute for Eco-Energy, KAIST, 335 Gwahangno, Yuseong-gu, Daejeon 305-701, Republic of Korea

<sup>3</sup>Department of Materials Science and Engineering, University of Wisconsin–Madison, Madison, Wisconsin 53706, USA

<sup>4</sup>Department of Materials Science and Engineering, Massachusetts Institute of Technology, 77 Massachusetts Avenue, Cambridge, Massachusetts 02139, USA

(Received 25 November 2008; published 30 January 2009)

First principles computations have been used to study Li mobility in the orthorhombic Li<sub>2</sub>NiO<sub>2</sub> structure with the *Immm* space group (I-Li<sub>2</sub>NiO<sub>2</sub>). Understanding Li mobility in I-Li<sub>2</sub>NiO<sub>2</sub> structure other than the conventional layered structure helps extend our understanding of Li transport in different oxide structures. Our results indicate that I-Li<sub>2</sub>NiO<sub>2</sub> is a reasonably good lithium ionic conductor with two-dimensional diffusion when the structure is maintained upon lithiation or delithiation. It is predicted that in the orthorhombic cell the activation barriers along the *b* axis and diagonal direction between *a* and *b* axes are fairly low, ensuring the facile lithium diffusion along those directions, while migration along the *a* axis is unlikely given the very high activation barrier (~2 eV).

DOI: 10.1103/PhysRevB.79.014305

PACS number(s): 66.10.Ed, 66.30.Ny, 66.30.Dn

## I. INTRODUCTION

There has been extensive research to develop a new positive electrode for rechargeable Li batteries with high specific capacity. Particular attention has been given to the Ni<sup>2+</sup>/Ni<sup>4+</sup> double redox couple, which has been shown to exchange two electrons in layered LiNi<sub>0.5</sub>Mn<sub>0.5</sub>O<sub>2</sub>,<sup>1–6</sup> LiNi<sub>1/3</sub>Co<sub>1/3</sub>Mn<sub>1/3</sub>O<sub>2</sub>,<sup>7,8</sup> Li(Ni<sub>x</sub>Li<sub>1/3–2x/3</sub>Mn<sub>2/3–x/3</sub>)O<sub>2</sub>,<sup>9</sup> LiNi<sub>2/3</sub>Sb<sub>1/3</sub>O<sub>2</sub>,<sup>10</sup> and spinel LiNi<sub>0.5</sub>Mn<sub>1.5</sub>O<sub>4</sub>.<sup>11</sup> Multielectron redox reaction can provide a way to overcome the capacity limitation caused by the usual limit of one electron per transition metal in an acceptable voltage range that applies to cations in most of cathode materials. Recently, we have reported the synthesis and electrochemical behavior of orthorhombic Li<sub>2</sub>NiO<sub>2</sub> with the *Immm* space group (I-Li<sub>2</sub>NiO<sub>2</sub>).<sup>12</sup> This structure can hold two Li per formula unit with Ni<sup>+2</sup> and exhibits a higher potential for the Ni<sup>+2</sup>/Ni<sup>+4</sup> redox couple compared to that in the layered form of Li<sub>2</sub>NiO<sub>2</sub>, which is derived from overlithiating LiNiO<sub>2</sub>. The higher potential was attributed to the structural aspect of relatively long Li-Li distance in I-Li<sub>2</sub>NiO<sub>2</sub>.<sup>12,13</sup> Even though we found that the undoped I-Li<sub>2</sub>NiO<sub>2</sub> gradually transforms to layeredlike structure upon cycling, therefore loses its capability to hold two lithium at high potential,<sup>13</sup> I-Li<sub>2</sub>NiO<sub>2</sub> structure provides a tactical idea how we can store more than two lithium per transition metal in a reasonable potential range in terms of a crystal structure.

The structure of I-Li<sub>2</sub>NiO<sub>2</sub> is rather unusual in that Ni is at the center of an oxygen rectangle and the oxygen atoms are not close packed. The most widely studied Ni oxide cathodes have layered or spinel structures, which both have octahedrally coordinated cations and close-packed oxygen sublattices. Li mobility is largely affected by (i) the oxygen arrangement, as Li needs to move through the polyhedron faces that oxygen atoms form, and (ii) the distribution of cations, as low activation diffusion paths generally require Li to remain as far possible from the other cations.<sup>14</sup> Hence, the diffusion mechanism of Li in this type of materials is ex-

pected to be significantly different from those in close-packed oxygen frameworks. In this paper we investigate the Li diffusion paths and their activation barriers in the I-Li<sub>2</sub>NiO<sub>2</sub> structure when the structure is assumed to be maintained upon lithiation or delithiation.

Our calculations indicate that I-Li<sub>2</sub>NiO<sub>2</sub> has two-dimensional diffusion paths and an overall Li diffusivity comparable to Li<sub>x</sub>CoO<sub>2</sub>, an excellent cathode material. In addition, we find that seemingly similar paths (one along the *a* axis and the other along the *b* axis) have very different activation barriers for Li migration due to the displaced Li position in the tetrahedral site.

## II. CALCULATION METHODS

All energies used for the Li mobility study are calculated with the spin-polarized generalized gradient approximation (GGA) (using the Perdew-Burke-Ernzerhof exchange-correlation parametrization<sup>15</sup>) to density-functional theory using a plane-wave basis set and the projector-augmented wave (PAW) method as implemented in the Vienna *ab initio* simulation package (VASP).<sup>16</sup> PAW potentials have been widely used in battery materials and shown the good predictive capability.<sup>17,18</sup> The Li diffusion constant is investigated following the approach used in Ref. 19. From our previous reports the activation barrier of lithium in oxide system is not sensitively dependent on the choice of either local-density approximation (LDA) or GGA.<sup>20</sup> Activation barrier calculations are performed with the nudged elastic band method<sup>21</sup> in supercells ( $3a \times 3b \times 1c$ ) containing 18 formula units (the primitive cell contains two formula units). The large supercell isolates the hopping atoms from their periodic images, providing an accurate answer for activation barriers in the dilute limit (the images of the migrating Li are more than 8 Å apart). All the activation barriers are determined in the dilute vacancy limit with 35 Li and 1 vacancy in the unit cell. The nudged elastic band method is used with eight replicas of the system which are initiated by linear interpolation be-

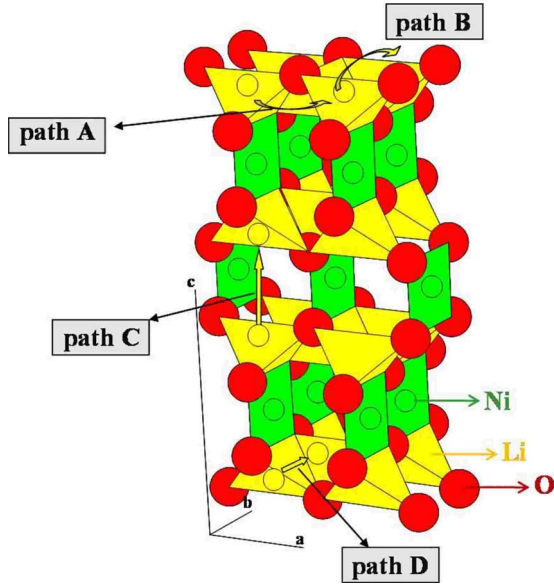


FIG. 1. (Color online) The orthorhombic  $\text{Li}_2\text{NiO}_2$  with  $Immm$  space group. Ni occupies the center of oxygen rectangle and Li occupies the tetrahedral sites. (Darker big circle: oxygen.)

tween the initial and final states of the path.<sup>22</sup> A global energy minimization is then performed with respect to ionic positions in each replica, whereby the coordinates of each replica are connected to those of its neighboring replicas in the interpolations sequence by a spring. The working of the algorithm can be compared to the tightening of an elastic band across a saddle point between two minima of the energy landscape. All lattice parameters are fixed at the fully relaxed lithiated values, but all the internal degrees of freedom are relaxed.<sup>23</sup> The approach taken in this work calculates the diffusion constant for Li assuming dilute vacancies and no constraints from electronic mobility. It is therefore only rigorously applicable in the discharged (Li rich) state and under the assumption of much faster intrinsic electronic than intrinsic ionic mobility.

### III. RESULTS & DISCUSSION

$\text{Li}_2\text{NiO}_2$  has an orthorhombic unit cell with oxygen arranged in a rectangular lattice plane as shown in Fig. 1. The

calculated lattice parameters are  $a=3.803 \text{ \AA}$ ,  $b=2.808 \text{ \AA}$ , and  $c=8.936 \text{ \AA}$ , which are within 2% of the experimental values.<sup>12</sup> The difference between the  $a$  and  $b$  lattice parameters is likely to arise from the Ni-O bonding and Ni-Ni repulsion. Ni binds with 4 oxygen along the  $[\text{NiO}_4]$  chain parallel to the  $b$  axis, resulting in a contraction in the  $b$  lattice parameter. Meanwhile, Ni faces other Ni along the  $a$  axis, without oxygen between them to provide electrostatic screening. This direct Ni-Ni interaction will be repulsive and increases the  $a$  lattice parameter. The oxygen rectangular planes are arranged along the  $c$  axis with  $AABB\dots$  stacking, where a  $B$  plane is shifted by  $[1/2 \ 1/2 \ z]$  from an  $A$  plane. Between two  $AA$  or  $BB$  planes, Ni occupies the center of an oxygen rectangle composed of two oxygen from above and two from below. The Li occupies two tetrahedral sites created between two different planes ( $AB$  or  $BA$ ). These tetrahedral sites are symmetrically equivalent mapped on to one another by an inversion center at the Ni site.

Based on the shortest distance between Li sites, there are four potential paths for Li hopping. They correspond to motion along a chain along the  $a$  axis (path A), motion along a chain along the  $b$  axis (path B), motion between oxygen planes along the  $c$  axis (path C), and motion along a diagonal between the  $a$  and  $b$  axes (path D). These paths are labeled in Fig. 1.

The path B requires hopping between two neighboring tetrahedral sites along the  $b$  axis. Li hops from one tetrahedral site to the other through the inside of a pyramid. Figure 2(a) shows the calculated activation energy along path B, where the abscissa is the distance along the path between Li in the initial and final states. The activation energy for Li to hop along this path is about 450 meV. The intrinsic Li diffusivity along this path can be estimated from the activation energy. Under the assumption of (i) a dilute hopping species, (ii) only nearest-neighbor hops among equivalent sites, (iii) noninteracting particles, and (iv) excluded volume (no two Li can occupy the same site), the diffusion constant can simply be represented as  $D=g\Gamma d^2$ ,<sup>24</sup> where  $\Gamma$  is the hopping frequency from a filled to a vacant site,  $d$  is the hopping distance, and  $g$  is a geometric factor relating to the number of nearest neighbors and the lattice topology. In general  $g$  is of order of 1 and will be ignored in this work.  $\Gamma$  can be shown to be approximately  $\nu^* \exp(-E_{\text{act}}/k_B T)$  using transi-

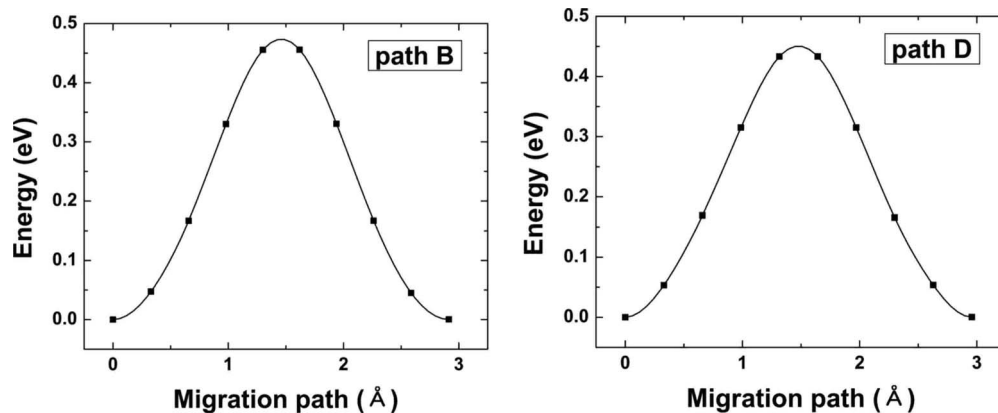


FIG. 2. Calculated energy along the different migration paths in Fig. 1(a) diffusion path B and Fig. 1(b) diffusion path D.

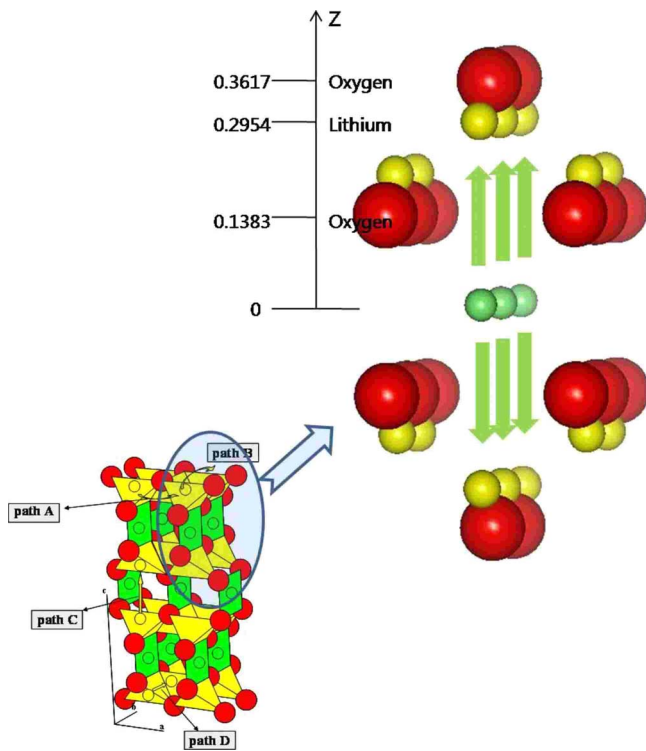


FIG. 3. (Color online) The tetrahedral Li is shifted away from the Ni due to the electrostatic repulsion. Along path A, the Li goes through the oxygen triangle that faces toward Ni, while along B, it moves through the oxygen triangle that faces away from Ni.

tion state theory,<sup>25</sup> where  $\nu^*$  is the attempt frequency and  $E_{\text{act}}$  is the activation barrier for the hop. The diffusion constant can therefore be estimated as

$$D = d^2 \nu^* \exp(-E_{\text{act}}/k_B T).$$

Assuming that  $d$  is approximately 3 Å, corresponding to the distance of a hop along path B, and  $\nu^*$  is about  $10^{13}$  Hz, which is in the range of phonon frequencies and consistent with typical values,<sup>26</sup>  $D$  for the path B can be approximated to be  $10^{-10}$  (cm<sup>2</sup>/s) at a temperature of 300 K. Considering that  $D$  for the commercially used  $\text{Li}_x\text{CoO}_2$  has been found to be within the range of  $10^{-13}$  to  $10^{-7}$  (cm<sup>2</sup>/s) at room temperature,<sup>27</sup> path B can be an acceptably fast Li diffusion path for cathode applications.

Similar to path B, path A involves hopping between two neighboring tetrahedral sites along the  $a$  axis by passing through the inside of an oxygen pyramid. Since path A is similar to path B, it might be expected to have a similar activation barrier. However, the calculated result shows that the activation energy for this path is over 2.5 eV implying that it is a nearly impossible diffusion path for Li. Figure 3 suggests a possible reason why these two similar paths have very different activation barriers. Since Li in the tetrahedral site sits right above the Ni site, there is a strong electrostatic repulsion. The large electrostatic repulsive forces push the Li up toward the edge of the tetrahedron. The first principles calculations show that the Li is shifted upward along the  $c$

axis from the regular position ( $z=0.25$ ) to  $z=0.2954$  in Fig. 3. This shift is fairly large considering the size of the tetrahedron. The motion of Li along the straight line interpolated between two Li tetrahedral sites along the  $a$  axis is prohibited since this route requires the Li to pass as near as 0.59 Å to the center of oxygen. Therefore, the motion along the  $a$  axis is shifted significantly downward along the  $c$  axis. However, this will also result in a strong electrostatic repulsion from the Ni below. The conflicting forces from the large oxygen atom and the strongly positive Ni cation, which cannot both be accommodated by the diffusing Li cause of the very large 2.5 eV barrier. This large barrier is in contrast to the case of motion along  $b$  axis. During the migration along the  $b$  axis, the Li does not get too close to the oxygen or need to take the shifted route that is unfavorable electrostatically.

The path C requires hopping through the Ni layer. Considering the Ni-Ni distance is only about 1.8 Å and without any screening by oxygen between them, Li is very unlikely to move into this direction. Therefore, no calculations have been performed for this path.

The path D involves Li hopping between edge-sharing Li sites along the diagonal direction between the  $a$  and  $b$  axes. In path D, Li is squeezed through the edge of tetrahedron. Figure 2(b) shows that the activation barrier is about 450 meV which is similar to the barrier along path B. Applying the same analysis as done above for path B, path D also gives a diffusion constant value of the order of  $10^{-10}$  (cm<sup>2</sup>/s). Paths B and D together will allow diffusion in the two-dimensional  $a$ - $b$  plane with a diffusion constant at 300 K on the order of  $10^{-10}$  (cm<sup>2</sup>/s). Paths B and D allow significant Li motion, making the orthorhombic  $\text{Li}_2\text{NiO}_2$  structure a two-dimensional ionic diffuser. Since path A does not provide energetically favorable diffusion paths, Li ions are expected to move in a zigzag manner only following the path B (along the  $b$  direction) and D (along the diagonal direction between  $a$  and  $b$  axes) in the plane. This kind of behavior can be contrasted with that in the layered structure where the Li motion in the plane is isotropic. In  $\text{I-Li}_2\text{NiO}_2$ , the difference in activation barrier along the  $a$  and  $b$  direction is attributed to the electrostatic repulsion from Ni which causes a significant shift in the Li position in the tetrahedron. This observation confirms the important relationship between the distribution of cations in the structure and the diffusion paths available. The observed diffusion mechanisms in  $\text{I-Li}_2\text{NiO}_2$  are also likely to apply for other structures with planar coordinated cations (such as  $\text{Li}_2\text{CuO}_2$  and  $\text{Li}_2\text{PdO}_2$ ) since the diffusion paths are likely to be dominated by gross features of the structure and electrostatics rather than element specific interactions.

In conclusions, we used first principles computations to study Li mobility in  $\text{I-Li}_2\text{NiO}_2$  structure.  $\text{I-Li}_2\text{NiO}_2$  structure is shown to provide a reasonably good lithium ionic diffusing structure (comparable to  $\text{Li}_x\text{CoO}_2$ ) with two-dimensional diffusion paths. Fairly fast Li motion is expected to occur along the  $b$  axis and the diagonal direction between  $a$  and  $b$  axes in this structure. The diffusion paths along other directions were prohibited by the strong electrostatic interaction with Ni.

## ACKNOWLEDGMENTS

This work was partly supported by the MRSEC Program of the National Science Foundation under Award No. DMR 02-13282, by the Assistant Secretary for Energy Efficiency and Renewable Energy, Office of Freedom CAR and Vehicle Technologies of the (U.S.) Department of Energy under

Contract No. DE-AC03-76SF00098, and Subcontract No. 6517748 with the Lawrence Berkeley National Laboratory. This work was also partly supported by the Korea Science and Engineering Foundation (KOSEF) grant funded by the Korea government (MEST) under Grant No. R01-2008-000-10913-0.

\*matlgen1@kaist.ac.kr

- <sup>1</sup>Z. Lu, D. D. MacNeil, and J. R. Dahn, *Electrochem. Solid-State Lett.* **4**, A191 (2001).
- <sup>2</sup>B. Ammundsen and J. Paulsen, *Adv. Mater. (Weinheim, Germany)* **13**, 943 (2001).
- <sup>3</sup>T. Ohzuku and Y. Makimura, *Chem. Lett.* **2001**, 744.
- <sup>4</sup>K. Kang, Y. S. Meng, J. Breger, C. P. Grey, and G. Ceder, *Science* **311**, 977 (2006).
- <sup>5</sup>J. Reed and G. Ceder, *Electrochem. Solid-State Lett.* **5**, A145 (2002).
- <sup>6</sup>K. Kang, D. Carlier, J. Reed, E. Arroyo, G. Ceder, L. Croguenec, and C. Delmas, *Chem. Mater.* **15**, 4503 (2003).
- <sup>7</sup>Z. Lu, D. D. MacNeil, and J. R. Dahn, *Electrochem. Solid-State Lett.* **4**, A200 (2001).
- <sup>8</sup>T. Ohzuku and Y. Makimura, *Chem. Lett.* **2001**, 642.
- <sup>9</sup>Z. Lu and J. R. Dahn, *J. Electrochem. Soc.* **149**, A1083 (2002).
- <sup>10</sup>X. Ma, K. Kang, G. Ceder, and Y. S. Meng, *J. Power Sources* **173**, 550 (2007).
- <sup>11</sup>Q. Zhong, A. Bonakdarpour, M. Zhang, Y. Gao, and J. R. Dahn, *J. Electrochem. Soc.* **144**, 205 (1997).
- <sup>12</sup>K. Kang, C. H. Chen, B. J. Hwang, and G. Ceder, *Chem. Mater.* **16**, 2685 (2004).
- <sup>13</sup>N. Imanishi, M. Nishijima, A. Hirano, T. Ikenishi, Y. Takeda, *Lithium Battery Discussion Electrode Materials*, Bordeaux-Arcachon, France, 2003, Abstract No. 99 (unpublished).
- <sup>14</sup>K. Kang and G. Ceder, *Phys. Rev. B* **74**, 094105 (2006).

- <sup>15</sup>J. P. Perdew, K. Burke, and M. Ernzerhof, *Phys. Rev. Lett.* **77**, 3865 (1996).
- <sup>16</sup>G. Kresse and J. Furthmuller, *Comput. Mater. Sci.* **6**, 15 (1996).
- <sup>17</sup>F. Zhou, M. Cococcioni, C. A. Marianetti, D. Morgan, and G. Ceder, *Phys. Rev. B* **70**, 235121 (2004).
- <sup>18</sup>F. Zhou, K. Kang, T. Maxisch, and G. Ceder, *Solid State Commun.* **132**, 181 (2004).
- <sup>19</sup>D. Morgan, A. Van der Ven, and G. Ceder, *Electrochem. Solid-State Lett.* **7**, A30 (2004).
- <sup>20</sup>A. Van der Ven and G. Ceder, *Electrochem. Solid-State Lett.* **3**, 301 (2000).
- <sup>21</sup>H. Jonsson, G. Mills, and K. W. Jacobsen, in *Classical and Quantum Dynamics in Condensed Phased Simulations*, edited by B. J. Berne, G. Ciccotti, and D. F. Coker (World Scientific, River Edge, NJ, 1998), p. 385.
- <sup>22</sup>S. Curtarolo, D. Morgan, and G. Ceder, *CALPHAD Comput. Coupling Phase Diagrams Thermochem.* **29**, 163 (2005).
- <sup>23</sup>A. F. Kohan, G. Ceder, D. Morgan, and Chris G. Van de Walle, *Phys. Rev. B* **61**, 15019 (2000).
- <sup>24</sup>R. Kutner, *Phys. Lett.* **81**, 239 (1981).
- <sup>25</sup>G. H. Vineyard, *J. Phys. Chem. Solids* **3**, 121 (1957).
- <sup>26</sup>A. Van der Ven and G. Ceder, *Phys. Rev. Lett.* **94**, 045901 (2005).
- <sup>27</sup>Y. I. Jang, B. J. Neudecker, and N. J. Dudney, *Electrochem. Solid-State Lett.* **4**, A74 (2001).